OG5.2-12

A MEASUREMENT OF THE ISOTOPIC COMPOSITION OF COSMIC RAY IRON

J. E. Grove*, E. R. Christian, R. A. Mewaldt, S. M. Schindler, E. C. Stone
California Institute of Technology, Pasadena, CA 91125 USA
A. Buffington
University of California at San Diego, La Jolla, CA 92093 USA
I. L. Rasmussen
Danish Space Research Institute, Lyngby, Denmark

*current address: E.O. Hulburt Center for Space Research, NRL,
Washington DC, 20375 USA

Abstract:

We present a new measurement of the isotopic composition of cosmic ray iron in the energy interval ~1550-2200 MeV/nucleon. The data were collected during the May 1984 flight of a balloon-borne spectrometer and show an average mass resolution of ~0.7 amu. The instrument employed the Cerenkov-Energy technique for mass determination. The observed $^{54}Fe/^{56}Fe$ ratio, $0.14^{+0.18}_{-0.11}$ at the top of the atmosphere, is consistent with a solar-system composition at the cosmic ray source. We also place an upper limit on the $^{58}Fe/^{56}Fe$ ratio at the top of the atmosphere of ≤ 0.07. Both are consistent with previous measurements at lower energies.

Instrument: The Caltech/DSRI High Energy Isotope Spectrometer Telescope (HEIST) is a balloon-borne mass spectrometer designed to measure the isotopic abundance of the cosmic rays from Ne to Ni ($10 \leq Z \leq 28$) at energies from ~1.5 GeV/nucleon to ~2.2 GeV/nucleon at the top of the atmosphere. Masses of particles which stop in the instrument are measured by the Cerenkov × Energy technique, while at higher energies masses of penetrating particles can in principle be measured by the Cerenkov × ΔE × Cerenkov technique (Buffington et al., 1983). Mass is given by the ratio of energy loss to velocity change,

$$M = \frac{\Delta E}{\Delta \gamma} .$$

The instrument consists of a stack of twelve NaI(Tl) scintillators bounded on each end by a Cerenkov counter and plastic scintillator (Buffington et al., 1983). The effective geometry factor varies with particle depth in the stack, ranging from 0.18 to 0.11 m^2sr. The layers of the NaI(Tl) stack provide a direct measurement of energy loss ΔE and also measure particle positions to an accuracy of ~0.5 cm for Fe (Grove, 1989; or Schindler et al., 1985).

The top Cerenkov counter contains a silica aerogel radiator with index of refraction $n \approx 1.1$, which corresponds to a threshold energy of ~1300 MeV/nucleon (Rasmussen et al., 1983). A calibration of the detector at the Bevalac in November 1982 showed that for the aerogel counter, the number of photoelectrons from a $Z = 1$, $\beta = 1$ particle was 18 ± 2. However, the light output was subsequently observed to degrade at an average rate of ~2% per month over a period of ~18 months, thus dropping by a factor of ~2 by the time of the flight (Grove, 1989). Note that this rate is ~2-4 times greater than that reported by other investigators (Poelz, 1986, and references therein). Although the precise source of the degradation remains unknown, it is presumed to have resulted from organic contamination of the aerogels, perhaps by the outgassing products of the $BaSO_4$ high-reflectivity paint used in the counters. Identical blocks of aerogel stored in a dessicator for a period of ~5 years do not show significant degradation.

The instrument was launched from Palestine, Texas, on 14 May 1984, and spent >35 hours at a mean float altitude of 6.0 g/cm^2 of residual atmosphere. The flight path ranged in vertical geomagnetic cutoff rigidity from ~4.1 to ~5.4 GV.

Analysis: The current analysis is restricted to Fe nuclei which stopped in the NaI(Tl) stack; thus only the Cerenkov × Energy technique was employed. Stopping events which

53

did not suffer charge-changing interactions were selected through a multi-step process. An initial rough selection of stopping Fe-group events $(24 \leq Z \leq 28)$ was achieved by the $dE/dx \times$ Energy method and by rejecting those events showing evidence of interaction daughters in the layers following the stopping point. A subsequent detailed comparison of response in the NaI(Tl) stack with the expected Bragg curve gave a charge measurement at several points in the instrument. A total of 32 stopping, non-charge-changing Fe nuclei were identified, while a Monte Carlo simulation predicted that 54 such events should have been observed (Grove, 1989). A number of uncertainties exist in the simulation, including the assumed spectrum at the top of the atmosphere and the filtering by the geomagnetic field, so that the disagreement may not be considered significant. Figure 1 shows a mass histogram of these events, along with the best fit discussed below.
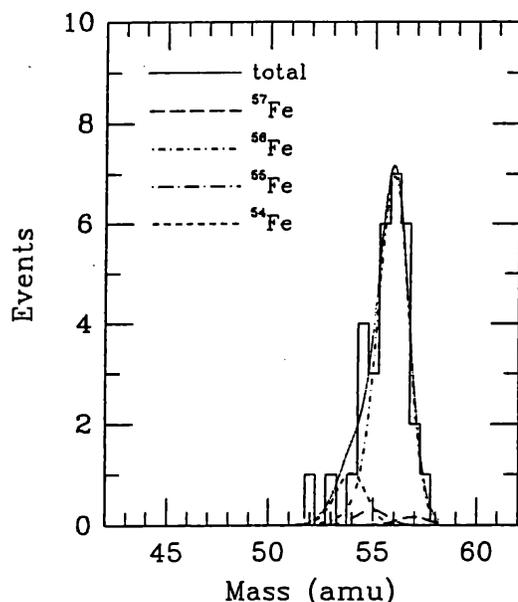

Figure 1: Mass histogram of the 32 Fe events, renormalized by the maximum-likelihood mass scale factor. The smooth curves are the calculated mass distributions for the isotopes of Fe.

The isotopic composition of Fe measured in the instrument is modified from that at the top of the atmosphere by nuclear interactions in the atmosphere and in the detectors. This includes a non-negligible number of neutron-stripping interactions in the NaI(Tl) stack, leading to a low-mass tail for a beam of a single isotopic species. We therefore used a maximum-likelihood technique to fit the measured masses with calculated mass distributions that accounted for these neutron-stripping interactions in the atmosphere and instrument. The calculated mass distributions were derived by convolving an assumed Gaussian resolution function with the result of a Monte Carlo calculation of the expected amount of neutron stripping. Cross sections on high-Z materials were derived from those of Webber (1987) on hydrogen. We have demonstrated that this procedure gives good agreement between the observed and the calculated mass distribution for ^{55}Mn using Bevalac calibration data (Grove, 1989).

Free parameters of the fit in Figure 1 were the ^{58}Fe/^{56}Fe and ^{54}Fe/^{56}Fe abundance ratios at the top of the atmosphere, along with the mass scale and mass resolution. We did not attempt to fit the abundances of ^{57}Fe and ^{55}Fe —instead we assumed a solar-system abundance of these isotopes at the cosmic ray source (GCRS) and propagated them to the top of the atmosphere as described below. Note that the solar-system abundance of the electron-capture nuclide ^{55}Fe is negligible, and thus its abundance at the top of the atmosphere is equal to the amount produced by the galactic propagation. We assumed that ^{55}Fe is stable once accelerated to cosmic ray energies because the probability of electron attachment from the ISM and subsequent decay is negligibly small at these energies (Grove, 1989).

The average mass resolution obtained was 0.67 ± 0.17 amu, consistent with theoretical estimates. The principal contributions to the mass resolution were from photoelectron statistical fluctuations, aerogel mapping uncertainties, and aerogel response normalization errors, all of which were increased by the degradation of the light yield of the radiator. The observed resolution from the Bevalac calibration done in November 1982 was 0.52 ± 0.01 amu for ^{55}Mn.

To interpret the measured composition, we propagated trial Fe isotopic abundances at the GCRS to the top of the atmosphere using a Leaky Box model that accounted for spallation interactions and deceleration in the ISM (assumed to be hydrogen), and also allowed unstable species to decay. Interaction cross sections were from Webber (1987). We used the source spectrum and rigidity-dependent mean escape length from Engelmann et al. (1985), and a mean mass density of 0.3 amu/cm^3 in the propagation volume. We used the force-field approximation of Gleeson and Axford (1968) to account for solar modulation, although its effect on composition at these energies is small.

Note that ^{54}Mn may decay by β^- emission to ^{54}Fe during propagation with a half-life which is rather uncertain. This decay can have a significant effect on the interpretation of the ^{54}Fe/^{56}Fe ratio observed at Earth (Grove et al., 1990). Assuming $\tau_{\frac{1}{2}} = 2 \times 10^6$ years (Koch et al. 1981) and a solar-system abundance ratio at the GCRS (i.e., ^{54}Mn absent and ^{54}Fe/^{56}Fe = 0.0632), the ^{54}Fe/^{56}Fe ratio at 1750 MeV/nucleon increases by $\sim$15% with respect to the ratio derived assuming that the weak decay does not occur.

Discussion: The table below summarizes our observations in the energy interval $\sim$1550-2200 MeV/nucleon at the top of the atmosphere, with 68% confidence intervals and 84% confidence upper limits. Note the large lower error bar for the observed ^{54}Fe/^{56}Fe ratio. Uncertainties in the propagation correction are large enough that our estimate of the ^{54}Fe/^{56}Fe ratio at the GCRS may also be considered to be an upper limit. Also listed for comparison are the solar system ratios (Anders and Ebihara, 1982).

Fe isotopic abundance ratios $\sim$1550-2200 MeV/nucleon			
Ratio	Top of Atmos.	GCRS	Solar System
^{54}Fe/^{56}Fe*	$0.14^{+0.18}_{-0.11}$	$0.12^{+0.18}_{-0.11}$	0.063
^{55}Fe/^{56}Fe	$\equiv 0.044$	$\equiv 0.0$	0.0
^{57}Fe/^{56}Fe	$\equiv 0.024$	$\equiv 0.023$	0.023
^{58}Fe/^{56}Fe	≤ 0.07	≤ 0.07	0.0032

*^{54}Mn decay $\tau_{\frac{1}{2}} \equiv 2 \times 10^6$ years.
$\rho \equiv 0.3$ amu/cm^3

To improve the upper limit placed on the ^{58}Fe/^{56}Fe ratio given above, we have combined our data with those of Mewaldt et al. (1980). We assume (conservatively) that one ^{58}Fe event was observed—the event with highest mass from the mass histogram in Figure 1, out of 26.5 ^{56}Fe from this data set and 27 ^{56}Fe from the Mewaldt et al. data set. The Poisson 84% confidence upper limit for the expected number of events when fewer than two are observed is 3.3 events, from which we derive a ratio of ^{58}Fe/^{56}Fe = 0.062. Our abundance ratios are consistent with previous measurements at lower energies (Tarlé et al. 1979, Mewaldt et al. 1980, Webber 1981, and Young et al. 1981).

Figure 2 summarizes five measurements of the ^{54}Fe/^{56}Fe abundance ratio at the GCRS as a function of energy. The data are plotted approximately at the average of their energy intervals at the top of the atmosphere or the orbit of Earth. All observed ratios have been propagated from Earth back to the GCRS by the same algorithm described above. The uncertainties of the current measurement are large due to the moderate mass resolution (comparable to that of Tarlé et al. and Young et al.) and low counting statistics. The dashed line indicates the solar-system ratio. In all cases, the observations are consistent with a solar-system source composition, although they do permit significant enhancements in ^{54}Fe and ^{58}Fe.
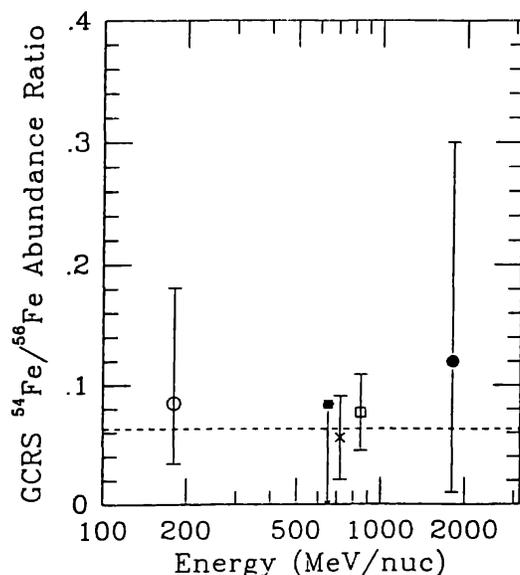
1990ICRC....3...53G

Figure 2: Calculated $^{54}Fe/^{56}Fe$ abundance ratios at the cosmic ray source. The data are plotted approximately at the average of their energy intervals at the top of the atmosphere or the orbit of the Earth. The dashed line marks the solar-system ratio. Open circle, Mewaldt *et al.*, (1980); filled square, Tarlé *et al.*, (1979); cross, Webber (1981); open square, Young *et al.*, (1981); filled circle, this work.

References:
Anders, E., and M. Ebihara, *Geochim. at Cosmochim. Acta*, **46**, 2363 (1982).
Buffington, A., *et al*, *Proc. 18th ICRC (Bangalore)*, **2**, 49 (1983).
Engelmann, J. J., *et al.*, *Astron. and Astroph.*, **148**, 12 (1985).
Gleeson, L. J., and W. I. Axford, *Ap. J.*, **154**, 1011 (1968).
Grove, J. E., *et al.*, *Proc. 21st ICRC (Adelaide)*, OG 8.3-5 (1990).
Grove, J. E., Ph.D. Thesis, California Institute of Technology (1989).
Koch, L., *et al.*, *Astron. and Astroph. (Letters)*, **102**, L9 (1981).
Mewaldt, R. A., *et al.*, *Ap. J. (Letters)*, **236**, L121 (1980).
Poelz, G., in *Aerogels*, ed. J. Fricke (Springer-Verlag: Berlin, 1986).
Rasmussen, I. L., *et al.*, *Proc. 18th ICRC (Bangalore)*, **8**, 77 (1983).
Schindler, S. M., *et al.*, *Proc. 19th ICRC (La Jolla)*, **2**, 103 (1985).
Tarlé, G., *et al.*, *Ap. J.*, **230**, 607 (1979).
Webber, W. R., *Proc. 17th ICRC (Paris)*, **2**, 80 (1981).
Webber, W. R., *Proc. 20th ICRC (Moscow)*, **2**, 463 (1987).
Young, J. S., *et al.*, *Ap. J.*, **246**, 1014 (1981).